Superconducting Quantum Computing

Spring 2018 Candidate Number: 6951Q

Part II Physics Research Review - University of Cambridge

Abstract

A Quantum Computer is a logical processor that uses intrinsically quantum properties - namely entanglement and superposition - to perform calculations. Theoretical work has shown that by harnessing this quantum behaviour certain problems can be solved exponentially faster than classically possible. In an effort to physically enact this, the last twenty years has seen concerted progress around the world towards the creation of an operational quantum computer.

Any number of systems could be used to create a quantum computer, just as anything from punch cards to semiconductors can be used to make a classical computer. We shall explore one leading implementation, superconducting circuits, tracing the development of state-of-the-art designs from their beginnings in the late nineties. In particular we shall discuss the Transmon, a conspicuously successful design that is now being worked into larger scale architectures. This is a rapidly progressing field with broad interest and I fully expect the current rate of development to continue for the foreseeable future.

1 Introduction

The impact of computers in science and beyond is self-evident; for one, only through computational modelling have many scientific problems become tractable. Yet in important areas our best computers struggle, for example, modelling many body quantum systems is a classically arduous task. Quantum Computers make use of quantum mechanics to perform information processing. Their fundamentally different mode of operating permits them to solve certain problems exponentially faster. Modelling quantum systems is, perhaps unsurprisingly, one of those problems - even a small quantum computer would drastically increase the complexity of systems we can model. This could expedite processes from drug design to material construction, but much like the unforeseen consequences of classical computers, the most exciting developments could be unplanned; who knows whether there is a quantum equivalent to meme culture?

This Research Review looks at one possible physical manifestation of a quantum computer, superconducting circuits. These present significant advantages over alternatives, foremost they are solid state so can be easily fabricated using standard lithographic techniques [1], and they can be controlled exclusively using microwave pulses [2]. Many leading quantum computation groups use superconducting circuits, not least IBM, and they appear one of, if not the, leading contender for future quantum computation.

We shall begin by laying groundwork regarding superconductivity and general Quantum Information concepts. Then we shall explore how superconducting circuits can be used to form the basic unit of quantum computation - the qubit. The past 20 years have seen a series of improvements in superconducting qubit design; we shall trace this development, culminating in the "Transmon" and its integration into a circuit QED read-out/manipulation set-up. Finally, we shall consider how to scale into more complex multi-qubit architectures and the challenges that must be overcome before full scale quantum computation becomes a reality.

2 Background Theory

2.1 A Crash Course in Superconductivity

A few details concerning superconductivity will be necessary for this review:

1. Many materials, when cooled to low temperatures, become superconducting; current flows within them without electrical resistance.
2. While superconducting a slight attraction arises between electrons such that they form loosely bound Cooper Pairs. The base unit of charge becomes twice the electron charge.
3. These Cooper Pairs are Bosons and can all exist at the lowest energy level. An entire superconductor can be described using one wavefunction; the only parameters necessary to describe this state are the amplitude and phase of this wavefunction.

2.2 The Qubit

The fundamental unit of quantum computation is the qubit, simply an isolated two level system:

$$|\psi\rangle = \alpha\,|0\rangle + \beta\,|1\rangle$$

The constants α and β are complex and thus there are four degrees of freedom. Two of these are constrained since first the wavefunction must be normalised ($|\alpha|^2 + |\beta|^2 = 1$) and second the global phase has no physical meaning - only the phase difference between α and β is measurable. We can then re-parametrise $|\psi\rangle$ in spherical polars as plotted in figure 1:

$$|\psi\rangle = cos\left(\frac{\theta}{2}\right)|0\rangle + sin\left(\frac{\theta}{2}\right)e^{i\phi}\,|1\rangle$$

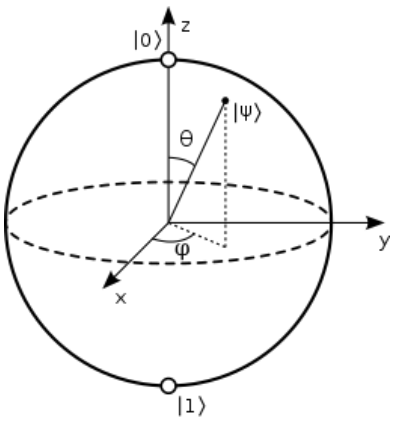

Figure 1: Qubit plotted on a Bloch Sphere - operations comprise rotating the qubit around the sphere. All pure states are represented by a point on the surface of the sphere, mixed states are those within the sphere. Source: Wikipedia.

2.3 Quantum Speedup

When solving many tough problems a classical algorithm is forced to use a brute force method, simply try many answers until you find the correct one. A set of qubits on the other hand can start in a superposition of many states, for example two qubits could be in the state $\frac{1}{2}(|00\rangle + |01\rangle + |10\rangle + |11\rangle)$. An operation performed on this superposition then acts on each part at the same time. By cleverly designing your algorithm the incorrect states within the superposition can destructively interfere and the correct constructively interfere. Upon completion of the algorithm and final measurement it becomes much more likely, or even deterministic, that the state collapses to the correct answer.

For certain problems this enables an exponential speed-up. A couple of semi-useful examples are Grover's search algorithm [3] for searching through databases and Shor's algorithm [4] to find prime factors. The Deutsch–Jozsa algorithm while not particularly useful is interesting as it deterministically returns the correct answer without requiring multiple runs [5]. There many other algorithms and yet more waiting to be discovered.

In the short term perhaps the most exciting prospect for quantum computing is the modelling of quantum systems. Qubits and molecules obey the same fundamental rules so it's not surprising that storing and manipulating such information is more efficient in a quantum than a classical computer. IBM's latest chip modelled a three atom system, BeH_2, and, though error prone, this was a serious proof of concept [6]. Supercomputers are limited to simulating 56 interacting qubits [7], quantum computers are beginning to reach this size [8] meaning soon we will not be able to predict their behaviour, signalling the reaching of genuinely virgin territory (a moment variously called quantum supremacy or quantum relevancy depending on whose side your on).

2.4 Coherence

Qubit states are tremendously fragile. Interactions with the environment can very easily degrade the state. The rate of information loss is quantified using two coherence times. T_1 is the bit flip time, the time for an excited state to decay to ground. Energy dissipating can cause this so must be avoided. The second, T_2, measures the time for the phase coherence to be lost, i.e. the time for $\frac{1}{\sqrt{2}}(|1\rangle + |0\rangle)$ to become $\frac{1}{\sqrt{2}}(|1\rangle - |0\rangle)$.

A qubit must achieve two competing objectives. First we must be able to manipulate and measure the qubit state easily; this requires strong coupling between our interventions and the qubit. Second the qubit must

be well isolated from noise in the environment, to limit decoherence. Superconducting circuits are mesoscopic systems containing many millions of particles - this makes coupling our interactions to the system relatively easy. Consequently removing or voiding environmental noise sources has been a key part of the superconducting qubit development process.

2.5 Error Correction

Classical bits are relatively easy to correct, the options are only 1 or 0 so if you measure 0.95 you can be pretty sure the bit is a corrupted 1. In addition sending multiple copies of the same data allows you to spot discrepancies by siding with the majority decision. In qubits you can do neither of these things; between measurements qubits occupy an analogue space described by two real numbers, and the no-cloning theorem [9] ensures that we cannot simply apply classical error correcting techniques. Further, directly checking for errors involves collapsing the state, making the whole process a waste of time.

Somewhat miraculously none of these problems are fatal, successful quantum error correcting techniques have been developed [10][11][12]. It is only through the existence of these protocols that physical quantum computing, complete with errors, can successfully operate, so it is perhaps worth briefly examining the basic scheme. To correct a bit flip error the qubit is stored in an entangled state with two additional ancilla qubits, $\alpha\,|1\rangle + \beta\,|0\rangle \rightarrow \alpha\,|111\rangle + \beta\,|000\rangle$. This entangled state is a simultaneous eigenstate of the Z_1Z_2 and Z_2Z_3 operators, where Z_i is the z Pauli Spin matrix acting on the i^{th} qubit:

$$\sigma_z = \begin{pmatrix} 1 & 0 \\ 0 & -1 \end{pmatrix}$$

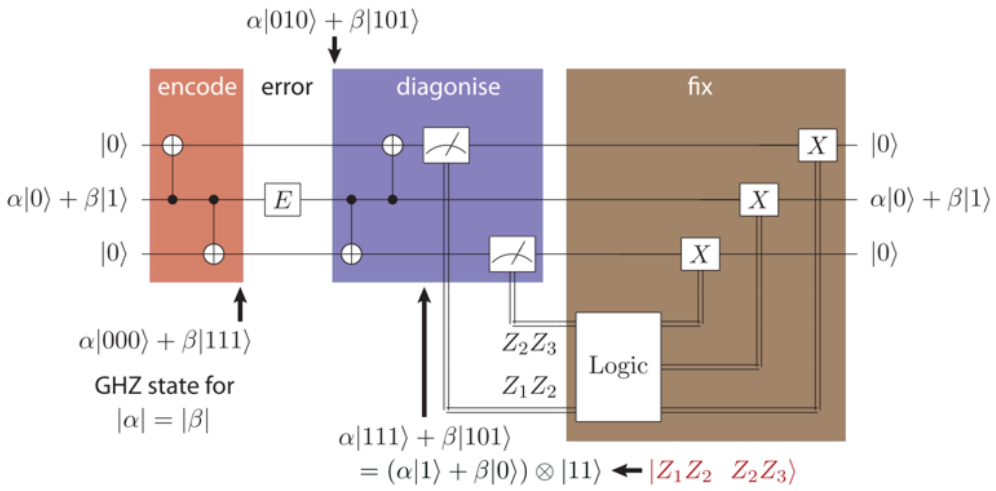

Figure 2: The bit flip correcting scheme. CNOT, or controlled not, gates are depicted by the dumbbell linking two qubit lines. A CNOT gate flips the state of the target qubit, the open crossed end of the dumbbell, only if the control qubit, the filled circle, is 1. The blue diagnose section of the circuit measures Z_1Z_2 and Z_2Z_3 through the operation CNOT gates and single qubit measurements. In the last, brown, section the error is corrected. Source: [13]

When the qubit is first encoded into an entangled state the eigenvalues of the Z_1Z_2 and Z_2Z_3 operators are 1. A bit flip error in any one of the three qubits will cause a unique change of eigenvalues, either Z_1Z_2, Z_2Z_3, or both, to -1. This allows you to identify the error and correct as appropriate, figure 2. This is not the same as copying the qubit, if any qubit were measured the set would collapse together. If, however, two errors occur the code is useless since it sides with the majority and assumes the one remaining correct qubit is in fact the error. Handling a second error in this format requires the inclusion of another two ancilla qubits.

Correcting phase flip error can be done by initially rotating the whole system by $\pi/2$ such that phases become bits. If an error occurs that is not a full π flip but some angle θ after the action of untangling CNOT gates, shown in the blue region of figure 2, the state would be:

$$|\psi\rangle = cos\left(\frac{\theta}{2}\right)(\alpha\,|0\rangle + \beta\,|1\rangle) \otimes |00\rangle + sin\left(\frac{\theta}{2}\right)(\alpha\,|1\rangle + \beta\,|0\rangle) \otimes |11\rangle$$

Upon measurement the ancilla qubits must either read 00 or 11, and as such we will have forced the system to decide whether no error or a full bit flip error has occurred. Hence we can correct an arbitrary qubit error and these ideas have been validated in small superconducting systems [14][15].

3 Superconducting Qubits

Our first implementation of an electrical qubit might be an LC circuit, simply a Quantum Harmonic Oscillator. As a qubit it has two major flaws. First electrical resistance dissipates energy and hence is a source of decoherence. This can be removed by cooling to very low temperatures where the circuit material, usually aluminium, is superconducting and the thermal excitations are much smaller than the transition energies.

Secondly, and more fundamentally, the energy levels are evenly spaced, figure 3a, meaning if we excite the system from the $|0\rangle$ to $|1\rangle$ state it will also be excited to the $|2\rangle$ state and onwards; significant leakage will occur into higher energy levels.

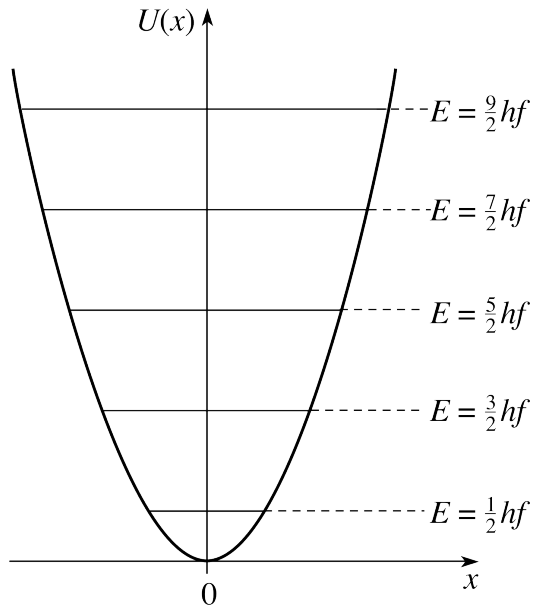

Figure 3a: Energy levels of a quantum harmonic oscillator. Source: Open University

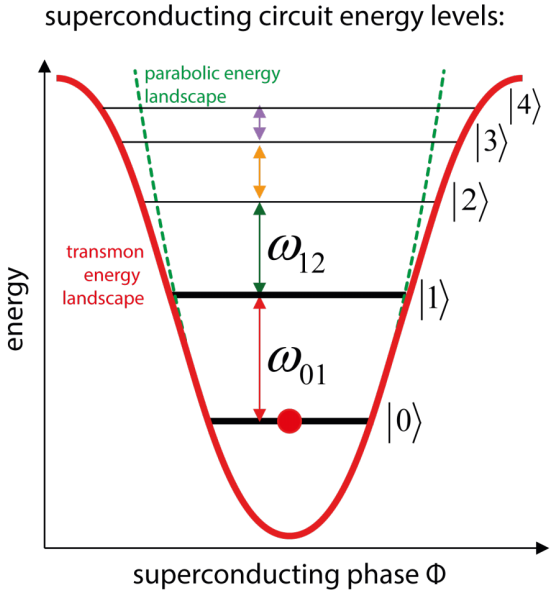

Figure 3b: Energy levels of the anharmonic Josephson Junction based curcuit, as a function of superconducting phase ϕ. Levels 0 and 1 form the qubit. Source: QUTEch Blog

In order to break the harmonicity we need a dissipationless non-linear circuit element. Fortunately just such an element exists, the Josephson Junction [16][17]. The junction consists of two superconductors separated by a narrow insulator, figure 4a . Cooper pairs are able to tunnel through the junction creating a dissipationless current, $I = I_c sin(\phi)$. In this equation ϕ is the phase difference between the superconducting wavefunctions on either side of the junction and I_c is the critical current, the maximum dissipationless current that can flow, a variable set by junction parameters such as barrier width. A voltage across the junctions obeys:

$$\hbar \frac{\partial \phi}{\partial t} = 2eV$$

Hence:

$$\frac{\partial I}{\partial t} = \frac{2eVI_c cos(\phi)}{\hbar}$$

This is an inductor equation with the non-linear inductance:

$$L_J = \frac{\hbar}{2eI_c cos(\phi)}$$

Further:

$$Energy = \int VIdt = \frac{\hbar}{2e} \int I_c sin\phi \frac{\partial \phi}{\partial t} dt = -E_J cos\phi$$

The energy's cosine dependence breaks the harmonicity producing an isolated pair of energy levels, perfect for a qubit, figure 3b.

Figure 4a: A real Josephson Junction. These are fabricated by oxidising an Aluminium wire and then laying another Aluminium wire above. Fortunately the oxidation of Aluminium is a self-terminating process, and the height at which the process stops is appropriate for the fabrication of Josephson Junctions. Source: Alexandre Blais.

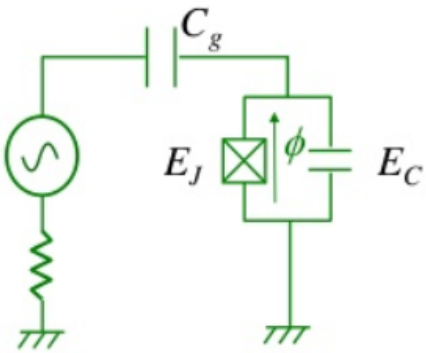

Figure 4b: Circuit Diagram showing the design of the Cooper Pair Box. The Josephson Junction is represented as a non-linear inductor in parallel with a capacitor, as, like most electrical elements, the junction has a capacitance. Source: Andreas Dewas.

The first superconducting qubit was the Cooper Pair Box (CPB) [18][19], which had nanosecond coherence times. This comprised a superconducting island connected via a Josephson Junction to ground and capacitively connected to an applied voltage, figure 4b. The voltage caused n_g cooper pairs to charge the capacitors, which have total capacitance $C_{Total} = C_J + C_g$ where C_J and C_g are the Josephson Junction and Gate capacitances respectively. In addition, n cooper pairs tunnelled through the junction, effectively neutralising some charge on the capacitor. Combining this capacitive energy with the Josephson Energy we derived earlier gives the CPB Hamiltonian:

$$H = \frac{2e^2}{C_{Total}}(n - n_g)^2 - E_J cos\phi = 4E_C(n - n_g)^2 - E_J cos\phi$$

n and ϕ are conjugate variables, $[n, \phi] = i$; this leads us to solve the equation $H|\psi\rangle = E|\psi\rangle$ with $n = \frac{\partial}{\partial\phi}$. The Matthieu functions are the solutions to this equation, i.e. the energy levels, and can be known to arbitrary precision, figure 5.

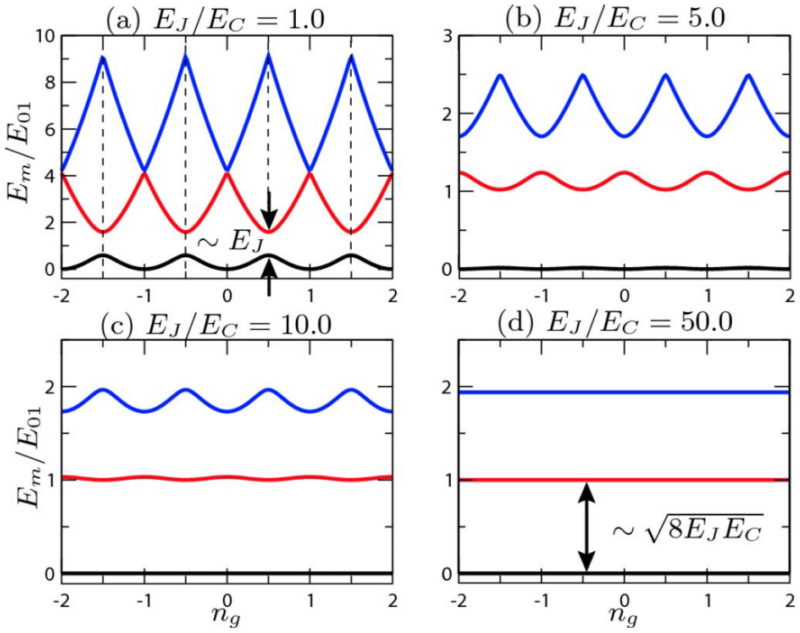

Figure 5: Shows the first three energy levels as a function of n_g for four different ratios of E_J/E_c. The periodicity arises from the repeated tunnelling of an extra cooper pair when the voltage reaches a threshold. For a pure charge qubit the energy levels differ in the number of cooper pairs which have tunnelled onto the island. Source: [20]

The applied voltage controls n_g and is set by the experimenter. However a good model for many noise sources is a small voltage applied across the box. These change n_g, n_g shifts the resonant energies and hence the system dephases. These noise sources are minimised if the system is biased at half integer n_g points where ω_{01}, the ground to excited transition frequency, is at extremum - the point shown by black arrows on figure 5. Here the system is first order impervious to noise. The second generation of superconducting qubits, the Quatroniums, used just such a biasing voltage and had extended coherence times of 100s of nanoseconds as a result [21]. A better solution however is highlighted by the behaviour at higher E_J/E_C, figure 5. This is the Transmon regime, which stretched coherence times into the microseconds [20][22].

The ratio E_J/E_C is set during fabrication and increasing it achieves the desired goal: The prominence of n_g charge noise decreases exponentially as $e^{-\sqrt{8E_J/E_C}}$, which can be seen from the flattening of the levels in figure 5, improving our systems coherence times. However we see also that the anharmonicity $(\omega_{01} - \omega_{12})$ is steadily decreasing. This could be a problem; the lower the anharmonicity the thinner in frequency space any pulse must be to prevent exciting higher energy levels. This means longer pulses and much slower processing.

This can, however, be tolerated. Firstly anharmonicity fortunately decreases polynomially, as $\sqrt{8E_J/E_c}$. We are therefore removing charge noise effects faster than anharmonicity. Secondly we can shape our pulses in frequency space to remove the ω_{12} frequency. (Theory [23], Experiential Validation [24]) This drastically improves processing time, figure 6.

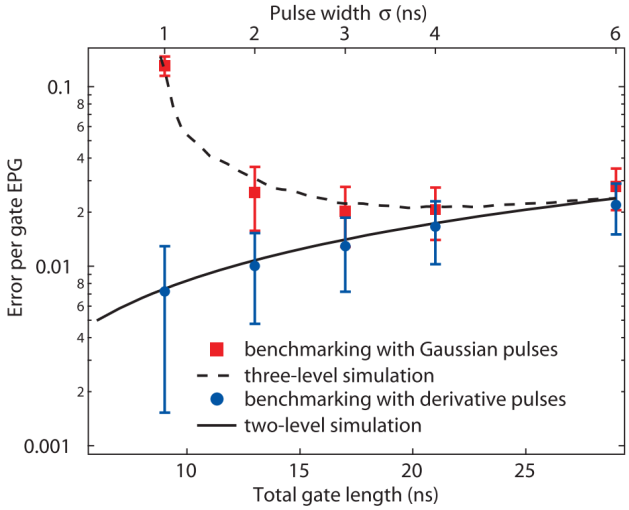

Figure 6: The error per gate as a function of gate length. Short Gaussian pulses excited the second transition causing significant errors. With derivative pulses, those we shaped to exclude ω_{12}, the fidelity is much improved. Source: [24]

3.1 Notes on Design

1. Physically the increased E_J/E_c ratio is implemented by wiring a large capacitance in parallel with the Josephson Junction.

2. Often two Josephson Junction are designed in parallel. This acts like a single junction except a flux can now thread the ring created. This is useful as it allows the experimenter to tune the resonant frequency of the qubit (proved here [25]), however leaves it vulnerable to flux noise.

4 Circuit QED

We concluded the last section with a qubit relatively impervious to environmental noise - the Transmon; we shall now explore the leading method for manipulating and measuring this qubit - cavity-qubit coupling or circuit QED [2][26], figure 7b. Within a cavity the strength of electric field zero point fluctuations scales inversely with cavity volume. Through a small cavity and the relatively large Transmon dipole moment, circuit QED provides strong interactions and fast gates.

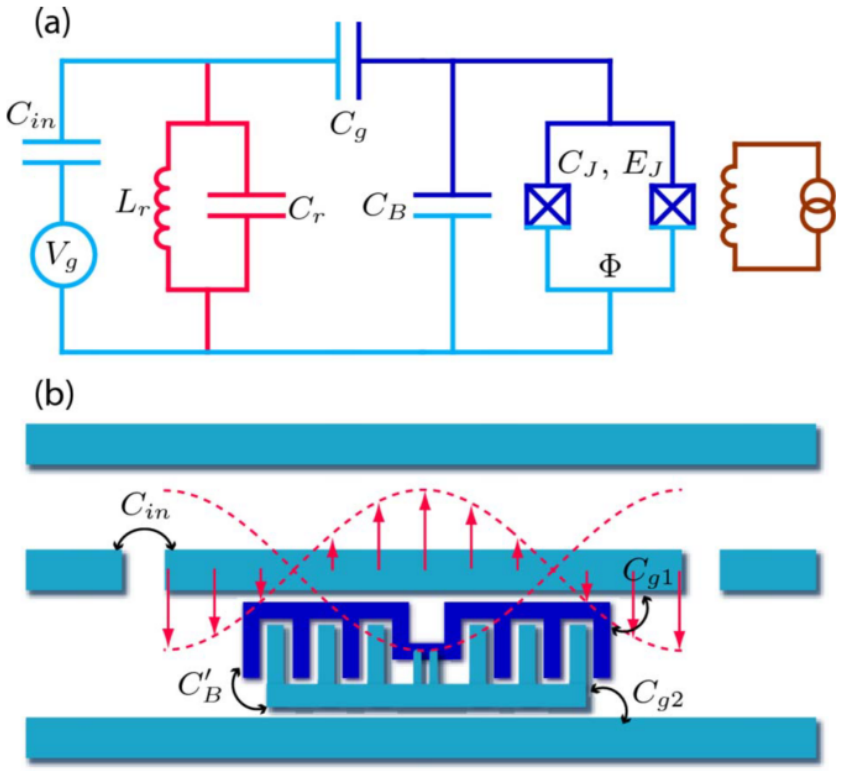

Figure 7: (a) Transmon Circuit Diagram. Included are a split Josephson Junction and a flux source to tune it (brown), the parallel capacitance to dampen the effects of the charge noise (C_B) and the cavity shown as a LC resonator circuit (red). The isolated section of superconductor is coloured dark blue.
(b) Circuit QED: a Transmon within a cavity. Also pictured, a constrained wavemode which acts as the applied voltage.
Source [20]

Cuts in a coaxial transmission cable define a Fabry-Pérot Étalon, figure 7b. Only wavelengths that have antinodes at each end of the cavity are transmitted well, thus the transmission spectrum is a series of sharp peaks. If the wavelengths are confined to a region surrounding just one peak we can model the cavity as an LC resonator, figure 7a.

To find the hamiltonian of this composite system we first note that in the Transmon regime n_g is unimportant. Then in the low ϕ limit of the bottom two energy levels the refined Transmon Hamiltonian becomes:

$$H \approx 4E_C n^2 + \frac{1}{2}E_J\phi^2 - \frac{1}{24}E_J\phi^4$$

Re-expressing this in qubit excitation creation and annihilation operators (b and $b^\dagger$) and applying the Rotating Wave Approximation:

$$H = (\sqrt{8E_C E_J} - E_C)b^\dagger b - \frac{E_C}{2}b^\dagger b^\dagger bb$$

Now we introduce the cavity using a second set of creation and annihilation operators (a and $a^\dagger$) and ω_r, the cavity frequency.

$$H = \omega_r a^\dagger a + (\sqrt{8E_C E_J} - E_C)b^\dagger b - \frac{E_C}{2}b^\dagger b^\dagger bb - g(a^\dagger - a)(b^\dagger - b)$$

The last term is an interaction mediated by g, the qubit-cavity coupling strength. We relabel the qubit transition frequency ω_{01}, limit the Transmon to only a two level system, and apply the Rotating Wave Approximation again to find:

$$H = \omega_r a^\dagger a + \frac{\omega_{01}}{2}\sigma_z + g(a\sigma_- + a\sigma_+)$$

Here the qubit excitations have been relabelled using Pauli Spin matrices. This is a Jaynes-Cummings Hamiltonian [27].

By setting the resonant frequencies of the qubit and the cavity to be significantly different photons will have trouble jumping from cavity to qubit, hence the coupling term will only be relevant in higher order perturbation theory. At the second order, in the limit $|\Delta| = |\omega_r - \omega_{01}| \ll g$, we find:

$$H \approx (\omega_r + \frac{g}{\Delta^2}\sigma_z)aa^\dagger + \frac{\omega_{01}}{2}\sigma_z$$

This hamiltonian comprises two resonators however the cavity frequency changes depending upon the qubit state! Hence measurement of the cavity frequency is also measurement of the qubit, figure 8.

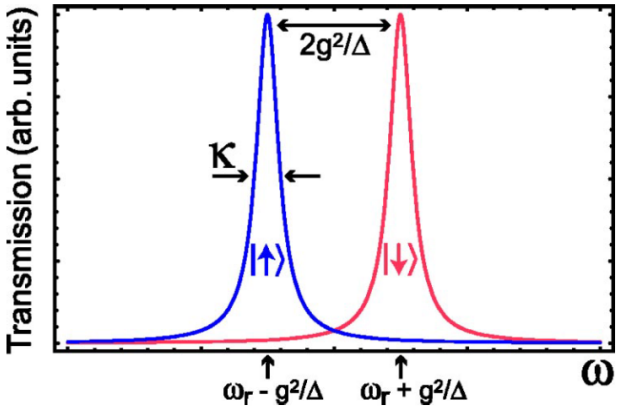

Figure 8: The dependence of cavity resonance on qubit state. κ is the cavity decay rate, this is inversely proportional to the cavity quality factor and the coherence time. Source [2]

We now have a method for measuring the qubit state, in order to exert universal control it is sufficient to be able to perform arbritrary single and two qubit gates [28] (manipulations of qubit state). Irradiating the system at the qubit transition frequency can be used for single qubit operations, as the cavity reflects most but not all off-resonance photons. Two qubit operations can be enacted in many ways, one scheme proceeds by tuning each qubit in and out of coupling with one shared resonator, the 'bus', allowing virtual photons to be exchanged via the bus [29], figure 9a. Universal gate schemes [30][31], two-qubit gates which don't require frequency tuning [32] and measurement of two qubit states using only one pulse [33], figure 9b, are amongst further developments, however we shall not explore this exciting progress in any more detail.

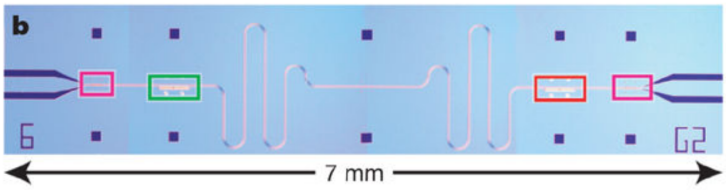

Figure 9a: Two Transmons, red and green boxes, coupled through a single resonator bus. Coupling of each qubit to readout is capacitive and the purple boxes are capacitors. Source [29]

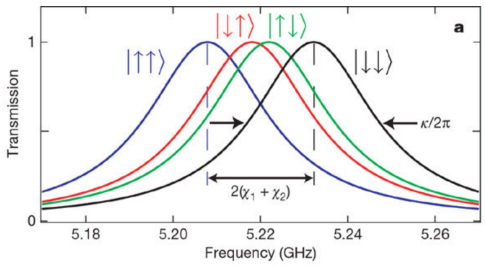

Figure 9b: Two Transmons dispersively change a shared bus' resonant frequency allowing distinction of all four two-qubit states from one measurement of cavity frequency. Source [29]

5 Extending the Transmon's Coherence Time

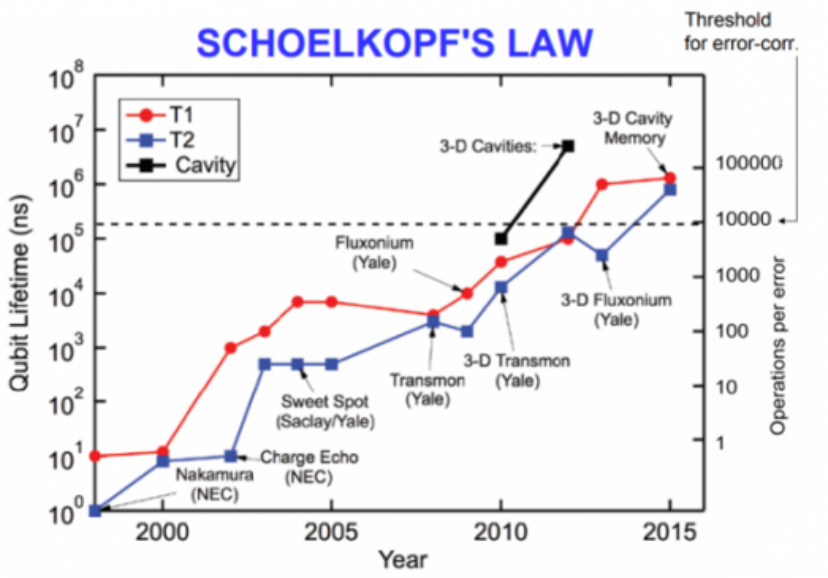

Figure 10: The steady improvement of coherence time. The right hand side gives the key parameter, operations per error, as long as this is high we need not be concerned with the absolute coherence time length. Source: Alexandre Blais

Lengthening coherence times remains a key priority, and their exponential growth has been labelled the Moore's Law of Quantum Computing, Schoelkopf's Law, figure 10. This improvement has largely been allowed by building a more comprehensive picture of the error sources, namely charge noise - which we modelled with an applied voltage, flux noise, material effects and residual coupling of the qubit to electromagnetic modes, intentional or not.

The largest recent improvement has been using 3D rather than planar cavities [22], figure 11a. Stray two level systems, such as dangling bonds, can couple to the cavity mode. Making the cavity three dimensional reduces the Electric field strength and hence reduces the coupling to the parasitic two level systems. However, by concurrently enlarging the Transmon and hence its dipole moment, the desired coupling can remain large. This led to $\approx 50\mu s$ coherence times which were further extended by excluding residual cavity photons [34].

Cavity modes alone have considerably longer coherence times than Transmons. Rather than combining them to make a 3D Transmon, the latest iteration uses very high quality factor cavity modes as a memory storage [35][36], figure 11b, extending coherence times to milliseconds.

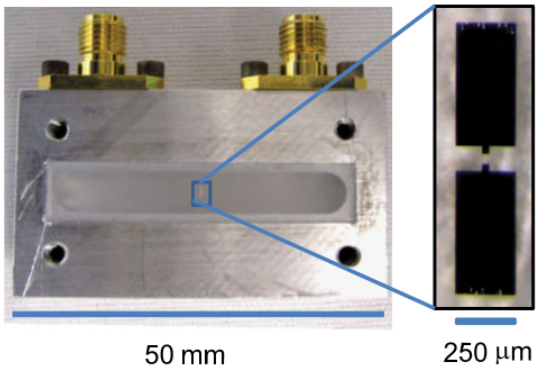

Figure 11a: 3D Transmon, an extended Transmon placed in a high Q 3D cavity. Source: [22]

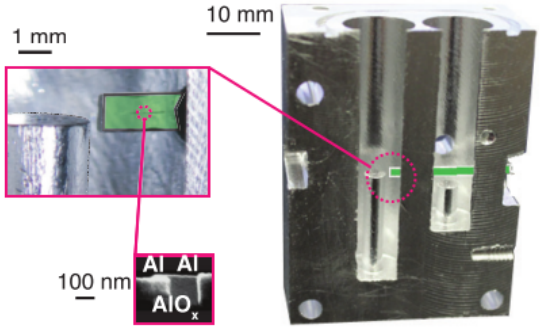

Figure 11b: 3D cavities with high quality factors serving as the memory for a Transmon qubit. Source: [36]

6 Scaling towards Quantum Computers

Designing scalable architectures for quantum computing presents additional challenges. Unintentional coupling between qubits arises, known as cross-talk, and systems larger than a microwave wavelength can support additional undesired electromagnetic modes - chip modes. Both of these can further constrain limited coherence times and gate fidelities. Currently there is a divergence of solutions, symptomatic of the nascent quality of the field.

One divergence is whether to have fixed frequency or tunable qubits. Tuning admits flux noise, additional circuitry and risks parasitic coupling of the qubit to a much wider range of systems as it flies through the frequencies; on the other hand single qubit gates work best when the qubits have very different frequencies, and multi-qubit gates when they have neighbouring frequencies. Achieving both criteria is only possible with tunable qubits.

IBM is arguably leading the pack, 16 and 7 qubit systems, figures 12a and 12b, are available for programming online and 20 and 50 qubit chips have been tested in their labs. These comprise planar Transmons coupled, both together and to readout, via buses. The qubits are fixed frequency and off resonance from the buses connecting them; two qubit gates are implemented by irradiating one qubit at the transition frequency of the other (Theory: [30]). These have been used to test error correction and molecular simulation methods [6].

The end goal appears to be a surface code [37], an error correcting code with a relatively high fault tolerance that requires only nearest neighbour interactions on a plane. Within these schemes many physical qubits are needed to define a single logical qubit, exactly how many depends on the fault tolerance of the qubit. Transmons are approaching the accuracy required for some surface codes [38] however the ratio of logical to physical qubits remains far too low. Pressing requirements therefore include extending coherence times and gate fidelities, such that this ratio increases to within the achievable realm, and 3D fabrication, which would stop the control circuitry from disrupting the plane of qubits [39].

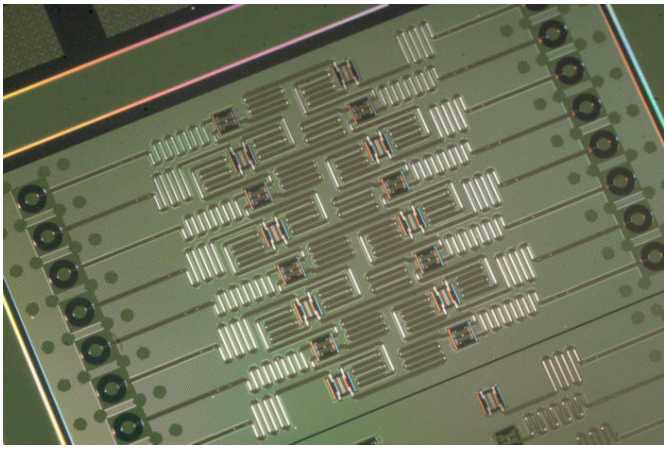

Figure 12a: 16 qubit chip, each with a readout resonator and two to three nearest neighbour couplings. Source: IBM

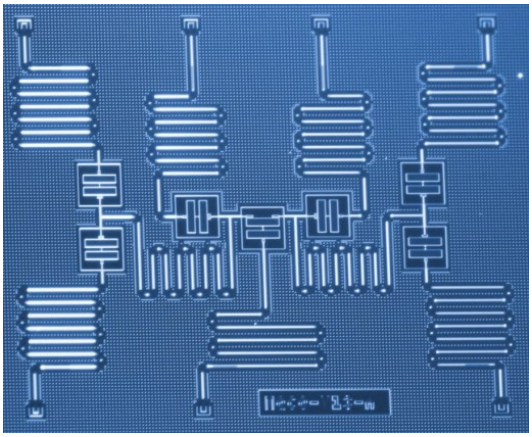

Figure 12b: 7 qubit chip, many qubits are coupled to the same resonator - before two qubit manipulations occur the others are decoupled. Source: IBM

Rigetti computing based in California propose a mixed system of fixed frequency Transmons and tunable Fluxoniums - a relatively flux noise impervious variety of qubit [40]. This network provides a short term alternative that possesses a few advantages over the large Transmon chips, for example a simple large scale planar structure. Whether it will drastically improve on IBM's work when it fails to directly answer chip modes or qubit coupling problems remains unknown.

A final and exciting proposal is the Multilayer Microwave Integrated Quantum Circuit (MMIQC) [41], figure 13. It counters chip modes and non-intentional qubit coupling by isolating separate modules within an electromagnetic shield. Each module contains circuitry of only limited complexity which is then connected to input, intermediaries and output as required through superconducting transmission lines. This builds heavily on the cavity memory storage system we discussed earlier [35][36] and incorporating these could help further extend coherence times. All this can be achieved using established techniques from the Micro-Electro-Mechanical Systems (MEMS) industry; preliminary steps have already proven fruitful at transferring these techniques to superconducting qubit systems [41].

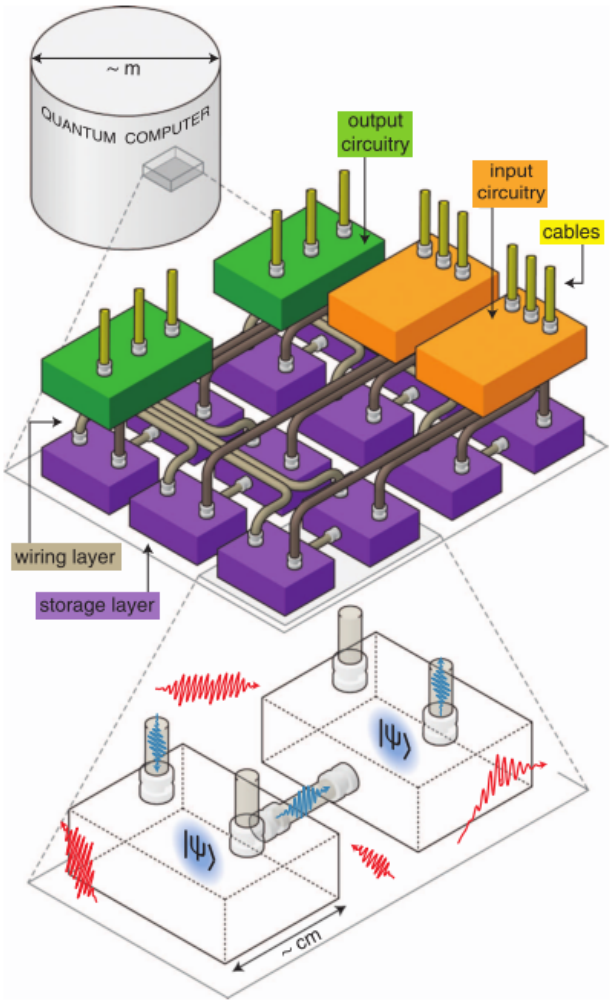

Figure 13: A schematic of the proposed MMIQC layout. Each box represents a module isolated from environmental noise (the red waves). While well isolated, the modules must be highly addressable; a perfect quantum state is no use if we cannot manipulate it. As such the connecting circuitry must be comprehensive. Source: [41]

7 Conclusions

In summary we have explored the leading superconducting qubit design, the Transmon in a circuit QED readout and manipulation set-up. In this system many of the criteria required for an operational quantum computer (the 'DiVincenzo Critera' [42]) have now been achieved thanks to a rapidly lengthening coherence time and comprehensive gate schemes. Scaling to larger systems will require novel solutions to emergent problems, however these appear surmountable. In particular we have examined perhaps the most exciting many qubit system, MMIQC, and this seems to suggest that intelligent architecture design will allow continued progress towards a large scale superconducting quantum computer.

To a greater or lesser extent this progress is mirrored by other quantum computational systems such as trapped ions or topologically braided quasi-particles; for example a recent annoucment described a 51 qubit ultra cold atom system [8]. Concurrently theoretical work continues apace in computer science and mathematics departments worldwide. This intense concentration of resources has led to a rich seam of developments that shows no sign of drying up. Quantum computation will be part of the future, what form it takes and the extent of its impact remain to be seen.

References

[1] Luigi Frunzio, Andreas Wallraff, David Schuster, Johannes Majer, and Robert Schoelkopf. Fabrication and characterization of superconducting circuit QED devices for quantum computation. In *IEEE Transactions on Applied Superconductivity*, 2005.

[2] A. Blais, R Huang, A. Wallraff, S. M. Girvin, and R. J. Schoelkopf. Cavity quantum electrodynamics for superconducting electrical circuits: An architecture for quantum computation. *Physical Review A - Atomic, Molecular, and Optical Physics*, 69(6):1–14, 2004.

[3] L Grover. Quantum Mehannics Helps in Searching for a Needle in a Haystack. *Phys. Rev. Lett.*, 79:325–328, 1997.

[4] Peter W. Shor. Polynomial-Time Algorithms for Prime Factorization and Discrete Logarithms on a Quantum Computer. *SIAM Journal of Computing*, 26(5):1484–1509, 1995.

[5] D. Deutsch and R Jozsa. Rapid Solution of Problems by Quantum Computation. *Royal Society of London Proceedings Series A*, 439:553–558, 1992.

[6] Abhinav Kandala, Antonio Mezzacapo, Kristan Temme, Maika Takita, Markus Brink, J. M. Chow, and J. M. Gambetta. Hardware-efficient variational quantum eigensolver for small molecules and quantum magnets. *Nature*, 549(7671):242–246, 2017.

[7] Edwin Pednault, John A. Gunnels, Giacomo Nannicini, Lior Horesh, Thomas Magerlein, Edgar Solomonik, and Robert Wisnieff. Breaking the 49-Qubit Barrier in the Simulation of Quantum Circuits. (1):1–24, 2017.

[8] Hannes Bernien, Sylvain Schwartz, Alexander Keesling, Harry Levine, Ahmed Omran, Hannes Pichler, Soonwon Choi, Alexander S. Zibrov, Manuel Endres, Markus Greiner, Vladan Vuletic, and Mikhail D. Lukin. Probing many-body dynamics on a 51-atom quantum simulator. *Nature*, 2017.

[9] William K. Wootters and W. H. Zurek. A Single Quantum Cannot be Cloned. *Nature*, 299(28):802 – 803, 1982.

[10] Raymond Laflamme, Cesar Miquel, Juan Pablo Paz, and W. H. Zurek. Perfect quantum error correcting code. *Physical Review Letters*, 77(1):198–201, 1996.

[11] Andrew M. Steane. Simple Quantum Error Correcting Codes. *Physical Review A*, 54(6):11, 1996.

[12] Peter W. Shor. Fault-tolerant quantum computation. 1996.

[13] M. D. Reed. Entanglement and Quantum Error Correction with Superconducting Qubits. *PhD. Thesis - Yale*, (May), 2013.

[14] Maika Takita, A. D. Córcoles, Easwar Magesan, Baleegh Abdo, Markus Brink, Andrew Cross, J. M. Chow, and J. M. Gambetta. Demonstration of weight-four parity measurements in the surface code architecture. *Physical Review Letters*, 117(21):1–8, 2016.

[15] M. D. Reed, L. Dicarlo, S. E. Nigg, L. Sun, L. Frunzio, S. M. Girvin, and R. J. Schoelkopf. Realization of three-qubit quantum error correction with superconducting circuits. *Nature*, 482(7385):382–385, 2012.

[16] B. D. Josephson. Tunnelling Supercurrents. *Proceedings of the IEEE*, 62(6):838 – 841, 1974.

[17] B. D. Josephson. Possible new effects in superconductive tunnelling. *Physics Letters*, 1(7):251–253, 1962.

[18] V. Bouchiat, D. Vion, P. Joyez, D. Esteve, and M. H. Devoret. Quantum Coherence with a Single Cooper Pair. *Physica Scripta*, T76(1):165, 1998.

[19] Y. Nakamura, Yu A. Pashkin, and J. S. Tsai. letters to nature Coherent control of macroscopic quantum states in a single-Cooper-pair box. *Nature*, 398(April):0–2, 1999.

[20] Jens Koch, Terri M. Yu, J. M. Gambetta, A. A. Houck, D. I. Schuster, J. Majer, A. Blais, M. H. Devoret, S. M. Girvin, and R. J. Schoelkopf. Charge-insensitive qubit design derived from the Cooper pair box. *Physical Review A - Atomic, Molecular, and Optical Physics*, 76(4):1–19, 2007.

[21] D. Vion, A Aasime, A Cottet, P. Joyez, H Pothier, C Urbina, D. Esteve, and M. H. Devoret. Mainpulating the quantum state of an electrical circuit. *Science*, 296(5569):886–889, 2002.

[22] Hanhee Paik, D. I. Schuster, Lev S. Bishop, G. Kirchmair, G. Catelani, A. P. Sears, B. R. Johnson, M. J. Reagor, L. Frunzio, L. I. Glazman, S. M. Girvin, M. H. Devoret, and R. J. Schoelkopf. Observation of high coherence in Josephson junction qubits measured in a three-dimensional circuit QED architecture. *Physical Review Letters*, 107(24):1–5, 2011.

[23] F. Motzoi, J. M. Gambetta, P. Rebentrost, and F. K. Wilhelm. Simple Pulses for Elimination of Leakage in Weakly Nonlinear Qubits. *Physical Review Letters*, 103(11):1–4, 2009.

[24] J. M. Chow, L. Dicarlo, J. M. Gambetta, F. Motzoi, L. Frunzio, S. M. Girvin, and R. J. Schoelkopf. Optimized driving of superconducting artificial atoms for improved single-qubit gates. *Physical Review A - Atomic, Molecular, and Optical Physics*, 82(4):2–5, 2010.

[25] David Isaac Schuster. Circuit Quantum Electrodynamics. *Thesis - Dissertation*, 2013.

[26] A. Wallraff, D. I. Schuster, A. Blais, L. Frunzio, R Huang, J. Majer, S Kumar, S. M. Girvin, and R. J. Schoelkopf. Strong coupling of a single photon to a superconducting qubit using circuit quantum electrodynamics. *Nature*, 431(7005):162–167, 2004.

[27] E. T. Jaynes and F. W. Cummings. Comparison of Quantum and Semiclassical Radiation Theories with Application to the Beam Maser. *Proceedings of the IEEE*, pages 89 – 109, 1963.

[28] Adriano Barenco, Charles H. Bennett, Richard Cleve, David P. Divincenzo, Norman Margolus, Peter Shor, Tycho Sleator, John A. Smolin, and Harald Weinfurter. Elementary gates for quantum computation. *Physical Review A*, 1995.

[29] J. Majer, J. M. Chow, J. M. Gambetta, Jens Koch, B. R. Johnson, J. A. Schreier, L. Frunzio, D. I. Schuster, A. A. Houck, A. Wallraff, A. Blais, M. H. Devoret, S. M. Girvin, and R. J. Schoelkopf. Coupling superconducting qubits via a cavity bus. *Nature*, 449(7161):443–447, 2007.

[30] Chad T. Rigetti and M. H. Devoret. Fully microwave-tunable universal gates in superconducting qubits with linear couplings and fixed transition frequencies. *Physical Review B - Condensed Matter and Materials Physics*, 81(13):1–7, 2010.

[31] P. J. Leek, S. Filipp, P. Maurer, M. Baur, R. Bianchetti, J. M. Fink, M. Göppl, L. Steffen, and A. Wallraff. Using sideband transitions for two-qubit operations in superconducting circuits. *Physical Review B - Condensed Matter and Materials Physics*, 79(18):1–4, 2009.

[32] J. M. Chow, A. D. Córcoles, J. M. Gambetta, Chad T. Rigetti, B. R. Johnson, John A. Smolin, J. R. Rozen, George A. Keefe, Mary B. Rothwell, Mark B. Ketchen, and M. Steffen. Simple all-microwave entangling gate for fixed-frequency superconducting qubits. *Physical Review Letters*, 107(8):1–5, 2011.

[33] S. Filipp, P. Maurer, P. J. Leek, M. Baur, R. Bianchetti, J. M. Fink, M. Göppl, L. Steffen, J. M. Gambetta, A. Blais, and A. Wallraff. Two-qubit state tomography using a joint dispersive readout. *Physical Review Letters*, 102(20):1–4, 2009.

[34] Chad T. Rigetti, J. M. Gambetta, Stefano Poletto, B. L T Plourde, J. M. Chow, A. D. Córcoles, John A. Smolin, Seth T. Merkel, J. R. Rozen, George A. Keefe, Mary B. Rothwell, Mark B. Ketchen, and M. Steffen. Superconducting qubit in a waveguide cavity with a coherence time approaching 0.1 ms. *Physical Review B - Condensed Matter and Materials Physics*, 2012.

[35] C. Axline, M. J. Reagor, R. Heeres, P. Reinhold, C. Wang, K. Shain, W. Pfaff, Y. Chu, L. Frunzio, and R. J. Schoelkopf. An architecture for integrating planar and 3D cQED devices. *Applied Physics Letters*, 109(4), 2016.

[36] M. J. Reagor, W. Pfaff, C. Axline, R. Heeres, Nissim Ofek, Katrina Sliwa, Eric Holland, C. Wang, J. Z. Blumoff, K. Chou, Michael J. Hatridge, L. Frunzio, M. H. Devoret, L. Jiang, and R. J. Schoelkopf. Quantum memory with millisecond coherence in circuit QED. *Physical Review B*, 94(1), 2016.

[37] A. G. Fowler, Matteo Mariantoni, J M Martinis, and A. N. Cleland. Surface codes: Towards practical large-scale quantum computation. *Physical Review A - Atomic, Molecular, and Optical Physics*, 2012.

[38] R. Barends, J. Kelly, A. Megrant, D. Sank, E. Jeffrey, Yu Chen, Y. Yin, B. Chiaro, J. Y. Mutus, C. Neill, P. J.J. O'Malley, P. Roushan, J. Wenner, T. C. White, A. N. Cleland, and J M Martinis. Coherent josephson qubit suitable for scalable quantum integrated circuits. *Physical Review Letters*, 111(8):1–5, 2013.

[39] J. M. Gambetta, J. M. Chow, and M. Steffen. Building logical qubits in a superconducting quantum computing system. *npj Quantum Information*, 3(1):0–1, 2017.

[40] Eyob A. Sete, William J. Zeng, and Chad T. Rigetti. A functional architecture for scalable quantum computing. *2016 IEEE International Conference on Rebooting Computing, ICRC 2016 - Conference Proceedings*, 2016.

[41] T. Brecht, W. Pfaff, C. Wang, Y. Chu, L. Frunzio, M. H. Devoret, and R. J. Schoelkopf. Multilayer microwave integrated quantum circuits for scalable quantum computing. *npj Quantum Information*, 2, 2016.

[42] David P. DiVincenzo. The Physical Implementation of Quantum Computation. *Fortschr. Phys.*, 48:771–783, 2000.